ONLINE SUPPLEMENT

PCSK9 Promotes Hypoxia-Induced Endothelial Cell Pyroptosis by Regulating Smac Mitochondrion-Cytoplasm Translocation in Critical Limb Ischemia

Supplemental Table

Supplemental Table 1 2

Supplemental Figures and Figure Legends

Supplemental Figure 1 3

Supplemental Figure 2 5

Supplemental Figure 3 6

Supplemental Figure 4 7

Supplemental Figure 5 8

Supplemental Figure 6 9

Supplemental Figure 7 10

Supplemental Figure 8 11

Supplemental Figure 9 12

Supplemental Figure 10 13

Supplemental Table

Supplemental Table 1. Characteristics of healthy subjects and CLI patients

Characteristics	Healthy subjects (*n*=20)	CLI Patients (*n*=20)	*p* value
Demographics			
Age (years)	63.3±11.3	67.4±12.9	0.29
Male sex [*n* (%)]	10 (50%)	10 (50%)	1.00
BMI, kg/m^2	22.5±3.0	22.1±2.9	0.71
Smoking [*n* (%)]	2 (10%)	3 (15%)	0.63
Blood pressure			
SBP (mmHg)	120.6±15.6	128.7±16.4	0.12
DBP (mmHg)	77.2±8.6	80.0±9.1	0.32
Metabolic indices			
Fasting serum glucose (mmol/L)	4.54±0.90	5.16±1.12	0.35
Total cholesterol (mmol/L)	4.83±0.85	5.71±1.48	0.006
Triglyceride (mmol/L)	1.13±0.54	1.96±0.75	0.001
HDL cholesterol (mmol/L)	1.23±0.25	0.91±0.26	0.004
LDL cholesterol (mmol/L)	2.85±0.65	4.42±1.53	0.0003

Categorical variables were shown as *n (%)*. Continuous variables are shown as mean ± SD. The differences between categorical variables were evaluated with chi-square test. The differences between continuous variables were analyzed using Student's *t*-test. CLI, critical limb ischemia; BMI, body mass index; SBP, systolic blood pressure, DBP, diastolic blood pressure; HDL, high density lipoprotein; LDL, low density lipoprotein.

Supplemental Figures and Figure Legends

Supplemental Figure 1

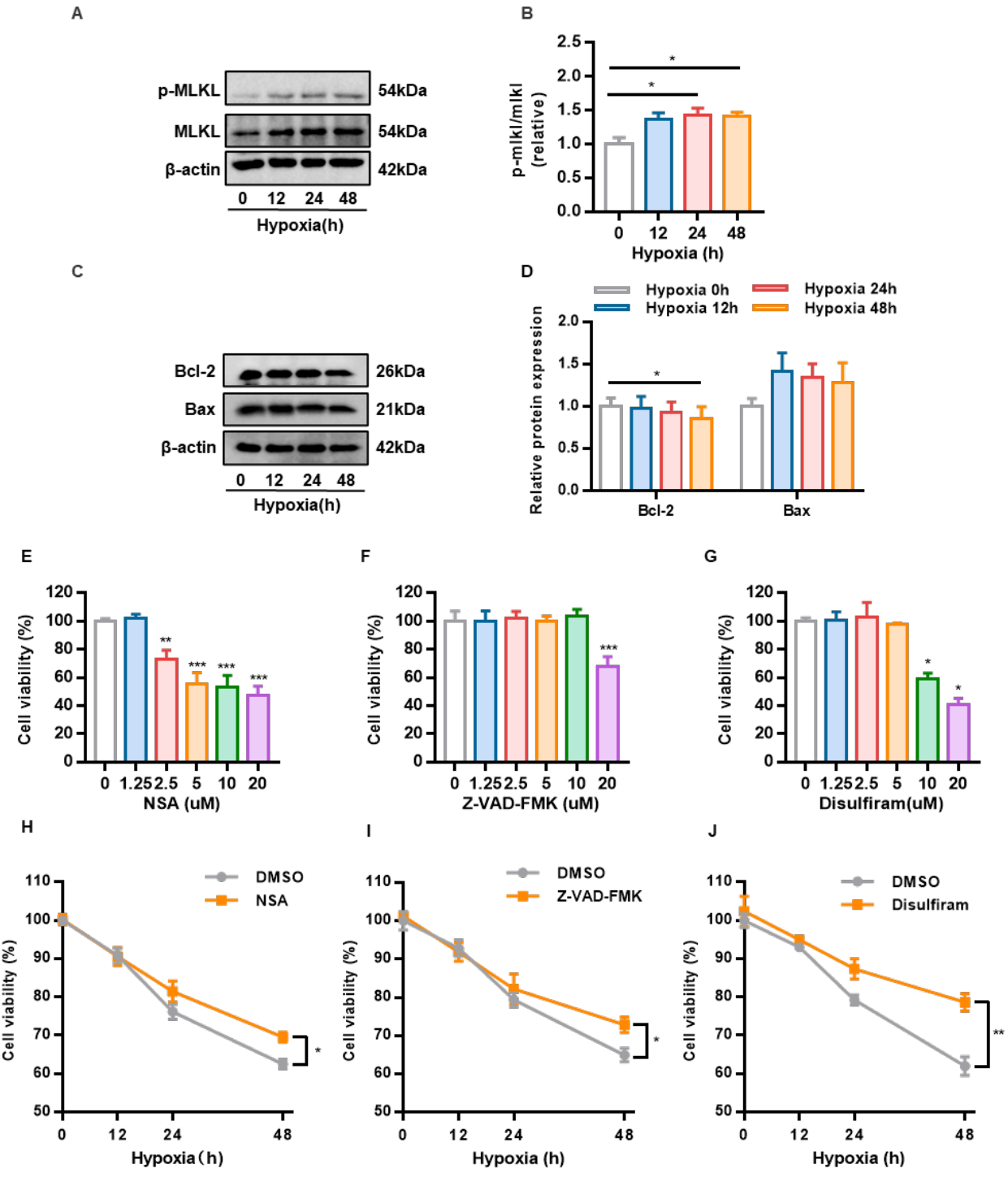

Supplemental Figure 1. Hypoxia induces HUVEC pyroptosis.

(A, B) Effect of hypoxia on necroptosis-related protein expression. (C, D) Effect of hypoxia on

apoptosis-related protein expression. (E-G) Effects of necroptosis inhibitor (Necrosulfonamide, NSA), apoptosis inhibitor (Z-VAD-FMK) and pyroptosis inhibitor (Disulfiram) on cell viability. (H-J) Effects of NSA, Z-VAD-FMK, and Disulfiram on cell viability under hypoxia. Data are expressed as mean ± SD. $n = 3$ per group, *$p < 0.05$, **$p < 0.01$, ***$p < 0.001$ compared to 0h in Data B and D and compared to 0 uM in Data E-G. Differences were compared to 48h DMSO in Data H-J. Data B, D and H-J were analyzed using repeated measures ANOVA. Data E-G were analyzed using one-way ANOVA analysis followed by Tukey's post-hoc analysis.

Supplemental Figure 2

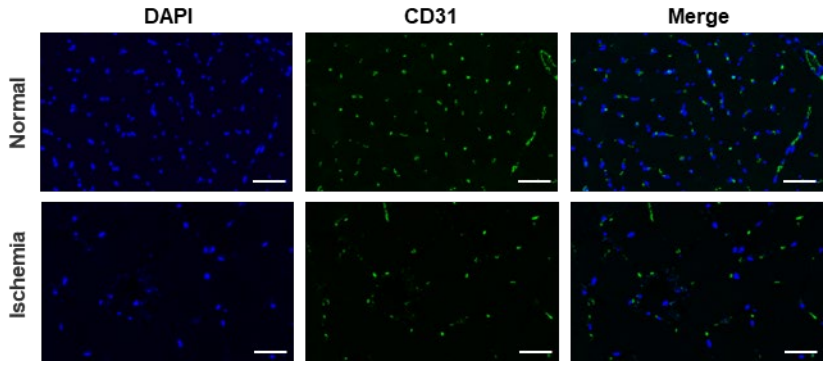

Supplemental Figure 2. The vessel density in the distal hypoxic muscle and proximal normoxia muscle.

The vessel density in the muscles (scale bar =50 nm).

Supplemental Figure 3

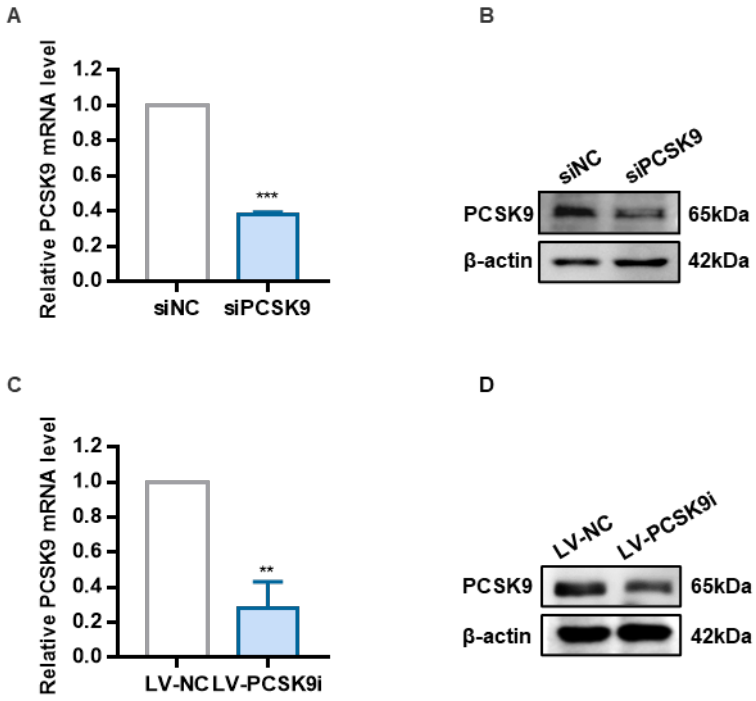

Supplemental Figure 3. Validation of PCSK9 knockdown.

(A, B) Validation of PCSK9 knockdown by siRNA in HUVECs via RT-qPCR and western blotting. (C, D) Validation of PCSK9 knockdown by lentivirus in HUVECs via RT-qPCR and western blotting. Data are expressed as mean ± SD. $n = 3$ per group, *$p < 0.05$, **$p < 0.01$, ***$p < 0.001$ compared to LV-NC. All data were analyzed using Student's unpaired *t*-test.

Supplemental Figure 4

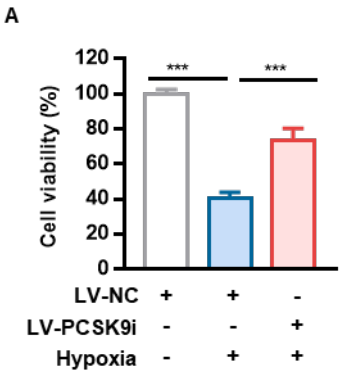

Supplemental Figure 4. Knockdown of PCSK9 increases cell viability during hypoxia.

(A) Cell viability detected by CCK8. Data are expressed as mean ± SD. $n = 3$ per group, $^{*}p < 0.05$, $^{**}p < 0.01$, $^{***}p < 0.001$ compared to hypoxia LV-NC group. Data were analyzed using one-way ANOVA analysis followed by Tukey's post-hoc analysis.

Supplemental Figure 5

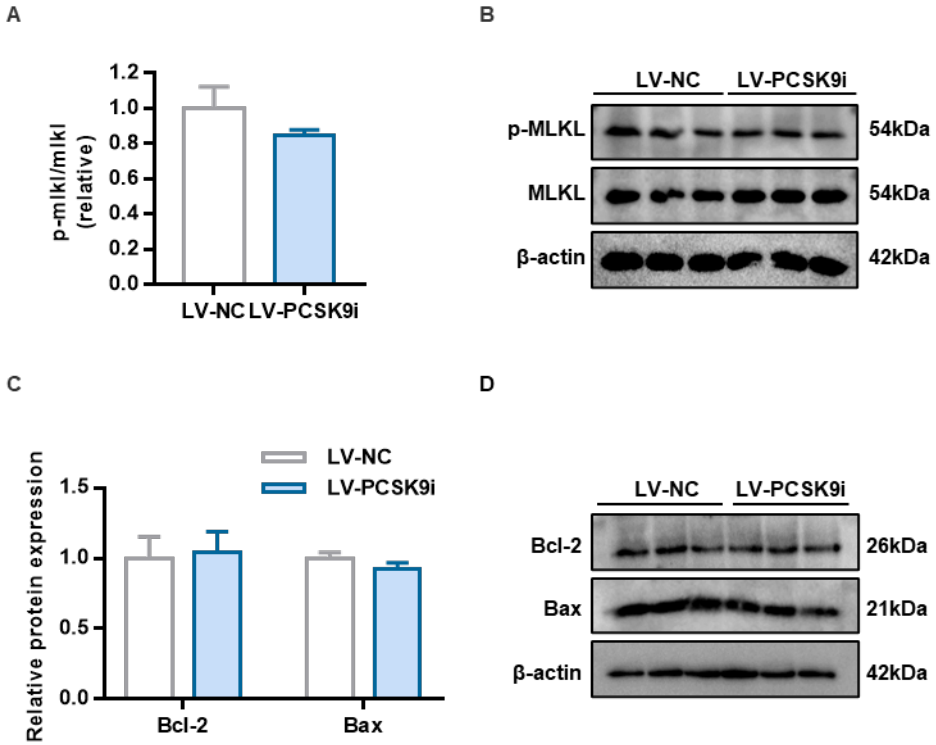

Supplemental Figure 5. Effects of PCSK9 knockdown on necroptosis and apoptosis during hypoxia.

(A, B) Effect of PCSK9 knockdown on necroptosis during hypoxia. (C, D) Effect of PCSK9 knockdown on apoptosis during hypoxia. Data are expressed as mean ± SD. $n = 3$ per group, $^{*}p < 0.05$, $^{**}p < 0.01$, $^{***}p < 0.001$ compared to LV-NC. All data were analyzed using Student's unpaired *t*-test.

Supplemental Figure 6

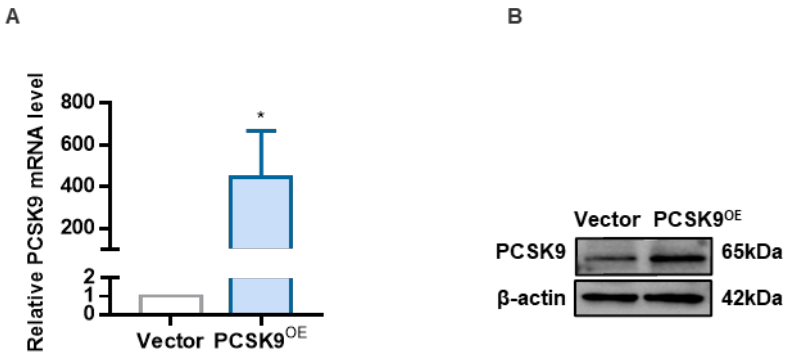

Supplemental Figure 6. Validation of PCSK9 overexpression.

(A, B) Validation of PCSK9 overexpression by plasmid in HUVECs via RT-qPCR and western blotting. Data are expressed as mean ± SD. $n = 3$ per group, $^{*}p < 0.05$, $^{**}p < 0.01$, $^{***}p < 0.001$ compared to Vector. Data were analyzed using Student's unpaired *t*-test.

Supplemental Figure 7

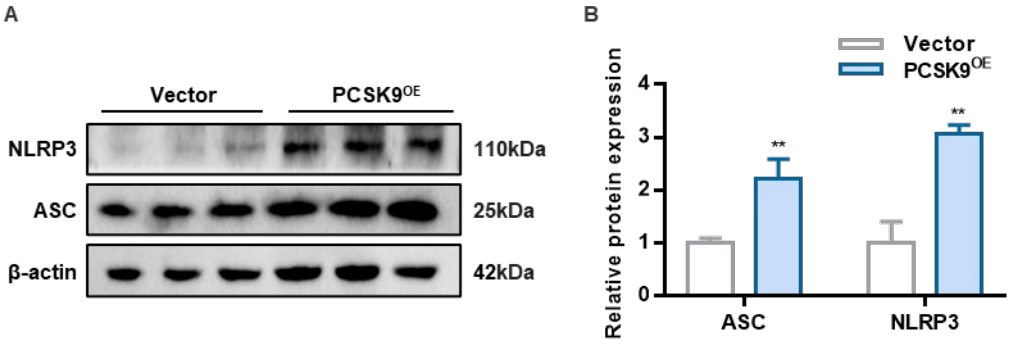

Supplemental Figure 7. Effects of PCSK9 activation on NLRP3 inflammasome.

(A, B) Western blot analysis of NLRP3 and ASC in PCSK9^{OE} HUVECs. Data are expressed as mean ± SD. $n = 3$ per group, $^{*}p < 0.05$, $^{**}p < 0.01$, $^{***}p < 0.001$ compared to Vector. Data were analyzed using Student's unpaired *t*-test.

Supplemental Figure 8

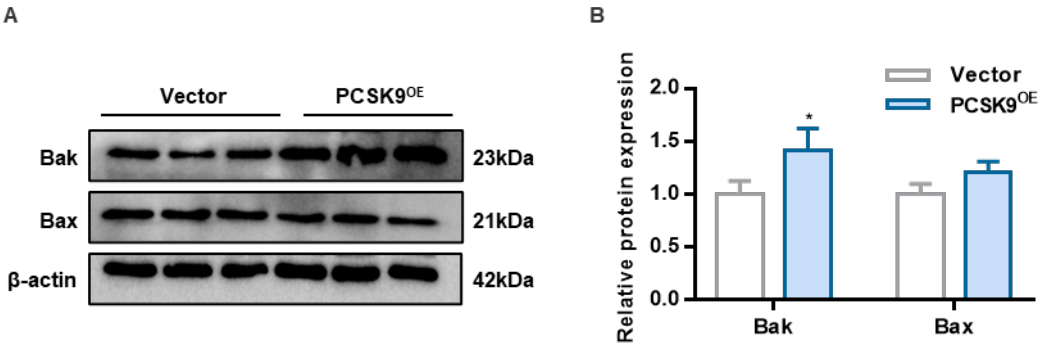

Supplemental Figure 8. Effects of PCSK9 activation on proteins related to mPTP opening. (A, B) Effects of PCSK9 activation on Bak and Bax. Data are expressed as mean ± SD. $n = 3$ per group, $^{*}p < 0.05$, $^{**}p < 0.01$, $^{***}p < 0.001$ compared to Vector. Data were analyzed using Student's unpaired *t*-test.

Supplemental Figure 9

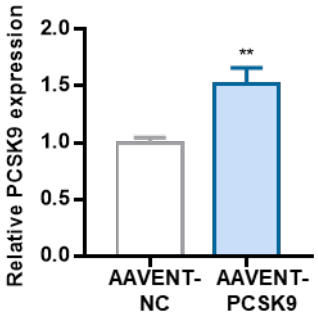

Supplemental Figure 9. The efficiency of PCSK9 overexpression induced by AAV injection.

Western blot analysis of PCSK9 level. Data are expressed as mean ± SD. $n = 3$ per group, $*p < 0.05$, $**p < 0.01$, $***p < 0.001$ compared to AAVENT-NC. Data were analyzed using Student's unpaired *t*-test.

Supplemental Figure 10

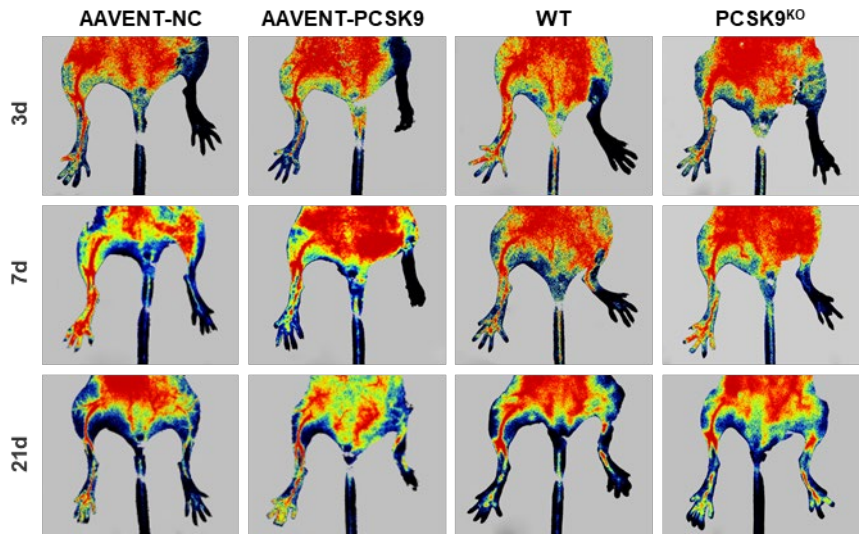

Supplemental Figure 10. PCSK9 inhibition improves blood perfusion in a female mouse lower limb ischemia model.

Blood perfusion in a female mouse lower limb ischemia model.